A sEMG-Driven Soft ExoSuit Based on Twisted String Actuators for Elbow Assistive Applications

A sEMG-driven Soft ExoSuit based on Twisted String Actuators for Elbow Assistive Applications

Mohssen Hosseini[1], Roberto Meattini[2], Andres San-Millan[1], Gianluca Palli[2], Claudio Melchiorri[2] and Jamie Paik[1]

***Abstract*—The scope of this work is to show the applicability of the Twisted String Actuators (TSAs) for lightweight, wearable and assistive robotic applications. To this aim, we have developed a novel surface electromyography (sEMG)-driven soft ExoSuit using the TSAs to perform both single and dual-arm elbow assistive applications. The proposed ExoSuit, with an overall weight of 1650 g, uses a pair of TSAs mounted in the back of the user, connected via tendons to the user's forearms to actuate each arm independently for supporting external loads. We confirm this new light-weight and customizable wearable solution via multiple user studies based on the biceps and tricep' sEMG measurements. We demonstrate that user's muscles can automatically activate and regulate the TSAs and compensate for the user's effort: by using our controller based on a Double Threshold Strategy (DTS) with a standard PID regulator, we report that the system was able to limit the biceps' sEMG activity under an arbitrary target threshold, compensating a muscular activity equal to 220% (related to a single arm 3kg load) and 110% (related to a dual arm 4kg load) of the threshold value itself. Moreover, the triceps' sEMG signal detects the external load and, depending on the threshold, returns the system to the initial state where it requires no assistance from the ExoSuit. The experimental results show the proposed ExoSuit's capabilities in both single and dual-arm load compensation tasks. Therefore, the applicability of the TSAs is experimentally demonstrated for a real-case assistive device, fostering future studies and developments of this kind of actuation strategy for wearable robotic systems.**

***Index Terms*—Wearable technology, Twisted String Actuation, sEMG, soft exoskeleton, soft robotics.**

I. INTRODUCTION

WEARABLE robots have been developed for a range of applications such as rehabilitation, assistance, as well as power augmentation and haptics. In order to assist or enhance the capabilities of the wearer, numerous actuation strategies have been used in these devices. One of the most common approaches is the usage of rigid links powered by traditional electric motors. In [1], a 12 DoF upper body exoskeleton that uses three electric motors to control 3 active DoFs is developed while in [2], an exoskeleton with an anatomically similar shoulder mechanism is presented. However, such rigid robotic systems require gear reductions which add to the overall weight on the human body as well as inertia on the motor [3]. Additionally, as the human joints are not perfectly rotational, kinematic incompatibility is observed in such devices, which can lead to discomfort. However, adding redundancy adds considerable complexity and weight to the system [2]. To circumvent these limitations, some studies have adopted a different approach by using soft materials and actuators in place of rigid links. These exosuits have low weight, apply well distributed forces on the body, and do not interfere with the natural movement of the wearer. The two broad categories of actuation in such exosuits are soft pneumatic actuators (SPAs) and cable-driven systems. In [4], a soft exosuit with pneumatic McKibben muscles for gait assistance is developed. SPAs are also used for assisting the elbow [5]. While they have been successful in controlled environments, since SPAs are powered by compressed air, a major challenge in their implementation is that of portability.

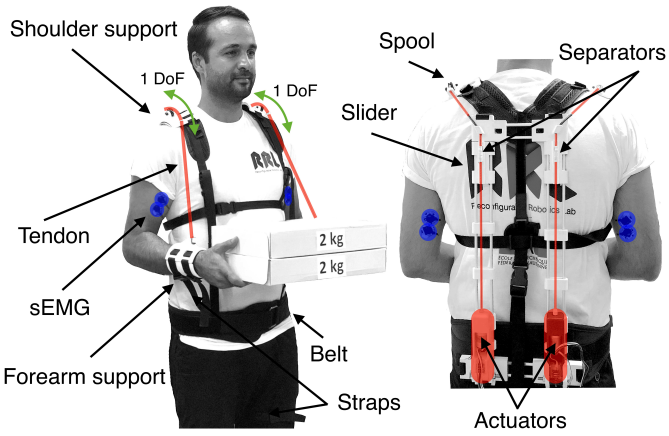

Fig. 1: Overview of the TSA-based ExoSuite.

Cable-driven actuators provide the advantages of a simple design, light-weight, high force output, reduced inertia added at the point of application and the possibility to have zero added impedance by introducing slack to the cable [8]. In [7]–[10] a cable-driven soft exosuit to assist walking after stroke has been developed, while [6] presents an exosuit for the elbow with a simple controller to provide assistance while removing gravitational forces. Such cable-driven systems consist of an electric motor and require gear reductions and pulleys for producing the necessary torques, increasing overall weight and inertia. A variation of cable-driven mechanisms is the Twisted String Actuator (TSA), in which an electric motor axially twists one end of a string, to produce linear pulling motion without need of additional transmission such as gears, belts or pulleys [11]. To better highlight the advantages of the TSA over pulley-based actuation, we newly report in Table. I a qualitative explicit comparison with benchmark studies presented in [7] and [6]. The TSA system is a very interesting solution for the implementation of compact, light-weight and low-cost linear transmission systems, since it delivers a very low inertia at the load side, allows the implementation of powerful

Manuscript received: October, 15, 2019; Revised February, 8, 2020; Accepted March, 20, 2020. This paper was recommended for publication by Editor A. Okamura upon evaluation of the Associate Editor K. Cho and Reviewers' comments.

[1] Reconfigurable Robotics Lab (RRL), École polytechnique fédérale de Lausanne(EPFL), Lausanne, Switzerland. (email: mohssen.hosseini@epfl.ch; andres.sanmillanrodriguez@epfl.ch; jamie.paik@epfl.ch)

[2] Dept. of Electrical, Electronic and Information Eng. (DEI), University of Bologna, Bologna, Italy. (email: roberto.meattini2@unibo.it; gianluca.palli@unibo.it; claudio.melchiorri@unibo.it)

TABLE I: Qualitative comparison between the proposed TSA and two selected benchmark pulley-based studies.

Study	Actuator	Motor type	Gear	Motor power	Actuator's weight (including supply)	Maximum task force
[6]	Pulley-based	Brushless motor	Geared	70 W	∼2 kg	∼100–250 N
[7]	Pulley-based	Brushless motor	Geared	200 W	∼6 kg	∼250 N
This work	TSA	DC motor	Gearless	30 W	∼0.85 kg	∼100 N

tendon-based transmission systems, by exploiting small-size gearless DC motors characterized by high speed, low torque and limited inertia which makes it very suitable for highly integrated robotic applications such as wearable robotics and exoskeletons. Furthermore, its slender structure makes it particularly suitable for wearable applications. With respect to conventional solutions, the main advantages of this actuation system consist in the direct connection between the motor and the tendon, very high reduction ratio, reduced friction and in the use of very small motors. Various application of TSA can be found in literature; an innovative anthropomorphic robotic hand "DEXMART", using 24 independent TSAs is reported in [12], while in [13] a light-weight exoskeleton device (Auxilio) for elbow and shoulder assistance is presented. ExoTen-Glove, a novel haptic interface for virtual reality is described in [14], as well as as a five fingered robotic hand [15] and tensegrity robots for space applications [16].

Toward the development of wearable rehabilitation and assistive systems, a soft ExoSuit for elbow assistive Applications based on TSA system is presented in this paper. The goal is to exploit a modular TSA system with combination of surface electromyography (sEMG) to develop a wearable assistive device in order to (i) to decrease the size, weight and mechanical complexity of the exoskeletons, such as pulleys and gears, to avoid complex regulation mechanisms; (ii) to implement an muscle-effort-adaptable and more comfortable system with removing all rigid joints attached to the human body. Several researchers exploited sEMG signals in the control of wearable assistive devices focusing on the estimation of joint torques during effort-demanding tasks by means of muscle activity measurements, mainly exploiting black box or model-based approaches [17]. However, not negligible drawbacks are present in torque estimation methods: complex task- and user-dependent algorithm calibrations are required, resulting in systems that are arduously usable outside laboratories. In the single-arm soft wearable robot of [6], the proposed controller implemented an elbow-joint-related gravity compensation,in which a constant posture of the upper arm was supposed. In [18], [19] and [20], antagonist-muscles-based machine-learning and model-driven techniques were used for joint torque estimations and adaptation to different users, requiring algorithm training/calibration phases. Additionally, in the aforementioned [6], [18], [19], [20], the measure of the entity of the assistance were exploited only *a posteriori*. Differently, the rationale of our work is based on directly exploiting the sEMG signals in closed-loop combining ease of use and effectiveness.

The main contributions of this paper are as follows:

- Demonstrate the applicability of the TSAs for wearable and light-weight assistive robotic devices;
- Development and test of a sEMG-based control strategy such that to exploit both biceps and triceps' sEMG activity to control the system and limit the human effort to an arbitrary threshold during load compensation tasks.
- Experimental protocol design to show the efficiency and capability of the entire assistive system to perform several single- and dual-arm load compensation tasks with adaption to different subjects and online-varying loads.

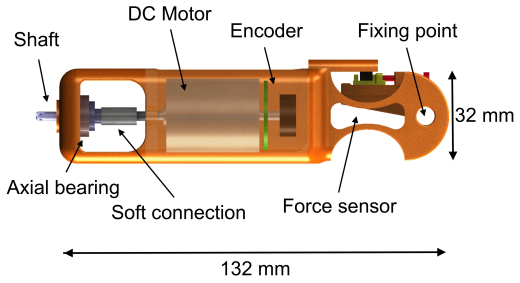

Fig. 2: Detailed view of the TSA module.

Our previous works on TSA focused on the novel actuator [21], and its potential application as a single arm support [22]. These studies serve a basis to the current manuscript where we present for the first time the following: a completely a brand-new hardware platform for bi-manual manipulations, extensive user studies using the wearable device for both single and bi-manual tasks, and incorporating triceps signals in the control scheme.

II. The TSA ExoSuit

A. The ExoSuit Design

Fig. 1 represents the overview of the proposed TSA-based ExoSuit. An independent pair of TSAs with an integrated force sensors are mounted in parallel on a light structure made of aluminium rods and ABS plastic on the back of the user. The strings twisted by the TSAs are present only on the back of the user, and then they are connected to the forearms supports through a shoulder path with tendons over a spool bearing to reduce the friction. The twisted string is connected to the tendons by a sliding elements: note that in this way, the initial state of the actuator length does not need to be adjusted for different users, since it is possible to adapt the length of the tendon. The twisted string, with the range of motion of 80 mm for this application, is connected to the tendons by a sliding element to prevent the twisting of the tendon itself. The forearm and shoulder supports are made of 3D printing ABS plastic integrating a soft material to improve the user's comfort. These supports can be adjusted by means of a pair of fabric straps. The structure is attached to the human body by fabric straps that could be easily worn and adjusted for different users. The overall weigh of the proposed system (excluding power supply), including actuators and electronic components is 1650 g.

B. TSA Module Structure

The designed TSA module fits very well with assistive application due to its light and compact structure and the ability of acting similarly to human muscles. Fig. 2 illustrates the schematic view of the TSA module with integrated force sensor which has been exploited for the implementation of the ExoSuit. The TSA working principle was presented and formalized in [11], and the TSA module design has been presented in details in [21], [22]. To measure the force applied by the load to the string, a force sensor based on optoelectronic components (OMRON EE-SX1131) is integrated into the actuation module. The optoelectronic sensor measures the frame deformation of a properly designed compliant structure integrated into the actuation module and converts the output voltage to the force [23], [24]. The advantages of using such sensor is a simplicity of the design, low-cost, the sensitivity and noise rejection. The TSA module consists of: a frame manufactured by 3D printing in ABS plastic, with the dimension of 132 mm (length), 32 mm (height), 32 mm (width), hosting electronics and mechanical components and with a connection to the ExoSuit frame; a low-cost, pass-through shaft 12 V DC motor with diameter of 25 mm equipped with a magnetic encoder for angular position sensing; an integrated force sensor composed by an axial-symmetric compliant double beam structure to measure the load force applied to the string; an output shaft supporting the load force through a combined bearing, in such a way that the DC motor transmits only the necessary torque to drive the TSA to the shaft; a flexible soft connection (silicon tube) to couple motor and shaft preventing misalignments; a pair of strings, each one with a diameter of 0.35 mm and composed by Dyneema fibers, connecting the motor module to the linear load. The total weight of the actuator is 135 g including all components. In this paper, regarding to our needs, the maximum force of the TSA is limited by the control at 140 N, while in reality the module could reach over 300 N, but the string would not hold beyond 140 N. The bandwidth of the TSA is between 2 and 3Hz, with an average life of approximately 20000 working cycles – please refer to [11] for more details.

C. Electronic Design and Control

To control the TSA modules, a pair of H-Bridges DRV8871 are employed to drive the 12 V DC motors from Pololu. These two H-Bridges are connected to an Arduino board that is controlled via serial communication from a host PC. In order to meet the real-time requirements of the system and read the encoders of both motors simultaneously, a pair of LS7366R counters keep track of each encoders' counts and provide the information to the microcontroller when requested via Serial Peripheral Interface (SPI). This avoids overloading the processor involved in servicing interruptions caused by reading both encoders at the same time.

III. sEMG-Based Control of the TSA ExoSuit

A. sEMG Data Acquisition

The acquisition of the sEMG signals is performed by the acquisition board *Cerebro*. The PCB is designed for wearable applications and is built in 6 layers technology. The high-performance Analog front End (AFE) acquires the sEMG signals and is connected with an ARM Cortex M4 Microcontroller. Finally, the data is transmitted via a Bluetooth interface to the control computer [25]. Two couples of differential electrodes are placed on the right and left upper arms of the subject, in proximity of the biceps brachii and triceps brachii (long head) muscle bellies. Note that the Cerebro board acquires raw sEMG signals, and before to use them in the ExoSuit control, a processing procedure is carried out as in our previous work [26]: *(i)* a 50 Hz notch filter, *(ii)* a 20 Hz high-pass filter, and *(iii)* the RMS value of the sEMG signal.

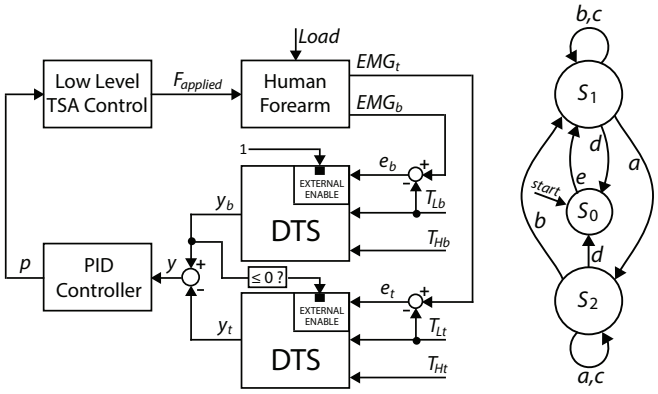

(a) (b)

Fig. 3: The block diagram of the sEMG-based controller. (a) Control for each single TSA module. (b) FSM of the DTS block behaviour, where: S_1 and S_2 are the *Enabled sEMG Error* and *Disabled sEMG Error* states, respectively, and a, b and c are the transition conditions corresponding to $EMG_i \geq T_{H,i}$, $EMG_i \leq T_{L,i}$ and $T_{L,i} < EMG_i < T_{H,i}$, respectively, with $i = \{b,t\}$; S_0 is the *Disabled* state, and e is the enabling condition corresponding to the external input of the DTS block equal to 1 and d is the disabling condition (external input equal to 0, see Fig. 3a).

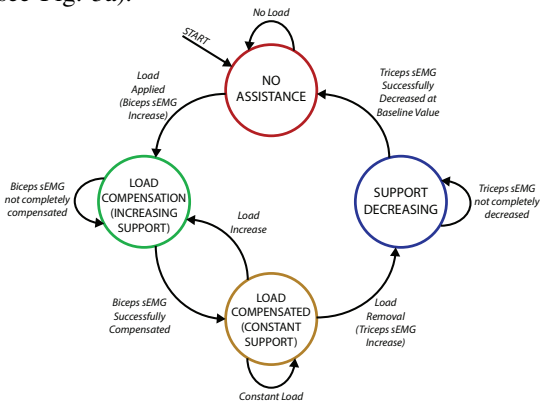

Fig. 4: Conceptual state machine reporting the load compensation functioning of the sEMG-driven TSA ExoSuit.

B. sEMG-Control for Load Compensation Tasks

We control the Exosuit based on the sEMG signals from the biceps and triceps (see Sec. III-A). The goal of controller is to provide an assistive torque to the elbow joint when a load is applied on the forearm.

Adaptation requirements to load variations: sEMG measurements from both biceps and triceps muscles are used in a combined manner to automatically achieve the behaviour reported by the conceptual state machine of Fig. 4. In particular, the TSA module must be able to adaptively compensate

TABLE II: Demographic data and threshold values for the subjects[1] involved in the experiment. $i = \{b,t\}$ (see Sec. III.)

Subjects	Gender	Age	Condition	$T_{L,i}$ $[mV]$	$T_{H,i}$ $[mV]$
U1	Male	37	Right-handed	0.134	0.203
U2	Male	34	Right-handed	0.114	0.173
U3	Male	29	Right-handed	0.164	0.246
U4	Male	32	Right-handed	0.13	0.195

additional effort produced by the subject's biceps in case of increasing loads. At the same time, we also consider that once the external (compensated) load is removed, the support force applied by the ExoSuit is rapidly reduced to avoid potential damages to the users (see details in the following controller paragraph.). The controller is developed for users standing with the upper arms parallel to the trunk, and the elbow joints both flexed at a fixed angle of 90° and then moving in order to perform a load lowering-lifting task.

Description of sEMG-based controller: A block diagram of the control system is outlined in Fig. 3. Referring to this figure, the force $F_{applied}$ that acts on the user's forearm and generate the assistive torque for the elbow is given according to a sEMG-driven control loop composed by a PID Controller which input is the difference between the outputs of two particular Double Threshold Strategy (DTS) blocks. Specifically, each DTS block is based on a sEMG error signal:

$$e_i = T_{L,i} - EMG_i, \;\; i = \{b,t\} \tag{1}$$

where the subscripts $\{b,t\}$ indicate the biceps and triceps muscles, respectively, $T_{L,i}$ is a lower threshold used as sEMG reference value and EMG_i is the sEMG signal measured from the muscles. Indeed, the output of the DTS block is given in accordance with the simple Finite State Machine (FSM) illustrated in Figure. 3b, in which S_1 represents the *Enabled sEMG Error* state and S_2 the *Disabled sEMG Error* state. According to the transition logic observable in Fig. 3b – when the load compensation task is in place – the output of the DTS block will be: *(i)* $y_i = e_i$ (state S_2) in case EMG_i surpasses a higher threshold value $T_{H,i}$ ($T_{H,i} > T_{L,i}$) or, conversely, *(ii)* $y_i = 0$ when (state S_1) EMG_i, decreasing, touches the lower threshold value $T_{H,i}$, or when (state S_0) the DTS block is disabled because the 'External Enable' input is set to 0. The implementation of such DTS is related to the advantage of a more reliable regulation of the sEMG signals with respect to single reference/threshold approaches, in which the presence of the variability of the sEMG cannot be handled without introducing instabilities and/or critical oscillations in the control action – for details refer also to [27].

In other words, applying a load on the user's forearm causes the sEMG of the biceps to increase and surpass the threshold $T_{H,b}$, activating the output y_b (i.e., $y_b = e_b$) and the related TSA. In this way, during the load compensation, $F_{applied}$ increases in accordance to the string length reference p_{ref}, in such a way that the biceps sEMG activity will decrease until it reaches the lower threshold $T_{L,b}$ (causing the transition to the S_1 state of FSM, i.e., $y_b = 0$.) This is possible because the user exploits the Central Nervous System (CNS) adaptation to the provided support. Moreover, it is important to underline the role of the triceps sEMG signal. Indeed, if the load compensated by the ExoSuit is removed, the triceps sEMG will increase to counteract the force support and keep the elbow position. This is exploited in the developed sEMG-driven loop: EMG_t will rise over the higher threshold $T_{H,t}$, activating the output y_t of the related DTS block (i.e., $y_t = e_t$) and causing a fast decreasing of the TSA-based $F_{applied}$, avoiding potential damages to the person. The rapid decreasing of the support force corresponds to an untwisting of the TSA's string, causing the system to rapidly come back to the initial state of no assistance. Note that this state is not related to the position of the user's forearm. This untwisting of the TSA can always be fast, because it is related only to the provided force. It is also important to consider that the user could co-contract biceps and triceps muscles, causing both to exceed the threshold value: in this case, the action of the DTS block related to the triceps' sEMG will be disabled (i.e., $y_t = 0$), since its 'External Enable' input will be equal to 1 only if $y_b = 0$. In this way, in case of co-contraction the user will inadvertently experience an increasing of the support force, causing the user to counteract this force, stopping to co-contract and using its triceps activity (as the support force is increasing during co-contraction, we claim that this condition is inevitable after a short time.) However, in our experiment we did not experience any biceps-triceps co-contraction by the subjects, since this had no functional reason to happen during the task of our protocol.

IV. EXPERIMENTAL EVALUATION OF THE PROPOSED DEVICE

A. Experimental Protocol

Selection of the Threshold Values: The threshold values $T_{L,b}$, $T_{L,t}$, $T_{H,b}$ and $T_{H,t}$ are determined for a particular subject by means of a simple calibration phase. In particular, the biceps' sEMG signal from the dominant arm of the user with the elbow flexed at 90° and with a load of 1 kg applied is recorded. Then, according to this, in the experiments carried out and reported in the next section, the thresholds were computed as

$$T_{H,b} = T_{H,t} = m_b - \sigma_b, \quad T_{L,b} = T_{L,t} = 2\,T_{H,b}/3, \tag{2}$$

where m_b is the mean value of the biceps' sEMG calibration recording and σ_b is the standard deviation computed over the same recording. The thresholds for the biceps are also used for the triceps for a reason of simplicity. Indeed, for the triceps sEMG signal, just a reasonable threshold that can easily be surpassed by the user' triceps sEMG signal when the load is removed is appropriate. This is also proved by the experimental results of Sec. IV-B. The threshold values for the subjects involved in the experimental testing are reported in Tab. II.

Load Compensation Tasks: The ExoSuit is worn by the subjects in order to perform two sets of experiments: single arm and dual arm. In the *single arm* experiments, the ExoSuit is tested only for the dominant arm of each subject (i.e. only one TSA is used), carrying out the compensation of three different loads applied on the forearm: 1 kg, 2 kg and 3 kg;

[1] We engaged four healthy participants. The experiments were performed in accordance with the Declaration of Helsinki.

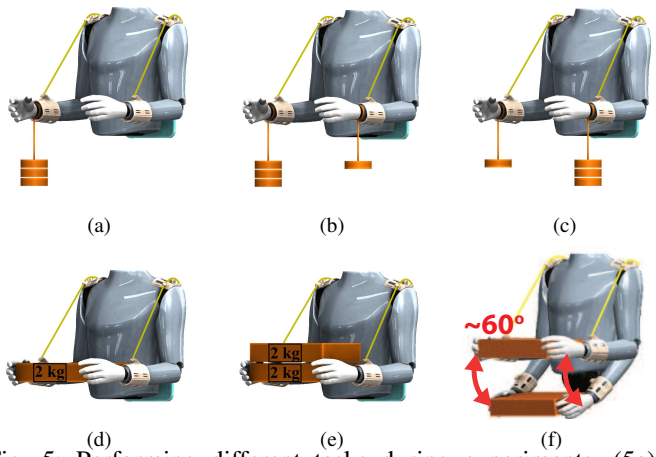

Fig. 5: Performing different tasks during experiments. (5a) applying 1 kg, 2 kg and 3 kg load on a single arm; (5b) and (5c) respectively, applying 3 kg on the right arm and 1 kg the left side, and vice versa; (5d) and (5e) holding a box of 2 kg and adding another 2 kg with both arms; (5f) 2 kg box lowering-lifting.

see Fig. 5a. In the *dual arm* experiments, three different tasks involving both users' arms were carried out. The first is the *decoupled compensation task*, with different loads applied on the two forearms and compensated at different instants of time. In detail, this task provided for two subjects (U1 and U2) the application of a 1 kg load on the right forearm and a 3 kg load on the left forearm, whereas vice versa for the remaining two subjects (U3 and U4) – refer Fig. 5b and 5c). The second dual arm experiment is the *simultaneous compensation task*, in which the two TSA modules provided assistance at the same time to support a box-like load that the subjects held with both arms. Importantly, here the load had been made to vary within the task execution, starting with a compensation of 2 kg and, thereafter, adding extra 2 kg to achieve a final compensation of 4 kg – refer to Fig. 5d, 5e. Finally, the third dual arm experiment is the *lowering-lifting task*, a dynamic task in which the load compensation assistance is exploited during repetitive, consecutive, lowering and lifting motions of a 2 kg box-like load. Please note that the subjects were asked to let their shoulder joint passive. Such request was attended by the subjects in a very natural manner, observing very small and smooth shoulder motions that did not require any stabilization of this joint.

B. Experimental Results

In order to better explain and report the fundamental aspects of the experimental results, first we refer to Fig. 6 as a *highlighted case*, regarding the dual arm experiment with the simultaneous compensation task (see previous Section) for the subject U1. Thereafter, single and dual arm experiment results are globally reported for all subjects.

Highlighted case: In Fig. 6, the behaviour and effects of the sEMG-based control strategy during the compensation task of the box-like load (see Fig. 1a, refer to Sec. IV-A) are shown for the subject U1. At the beginning of the task (time $t = 0s$) the ExoSuit control system was turned off (gray-coloured zone in Fig. 6): a single box of 2 kg was held by the subject (see Fig. 5d) and the sEMG signal of the biceps muscle was over

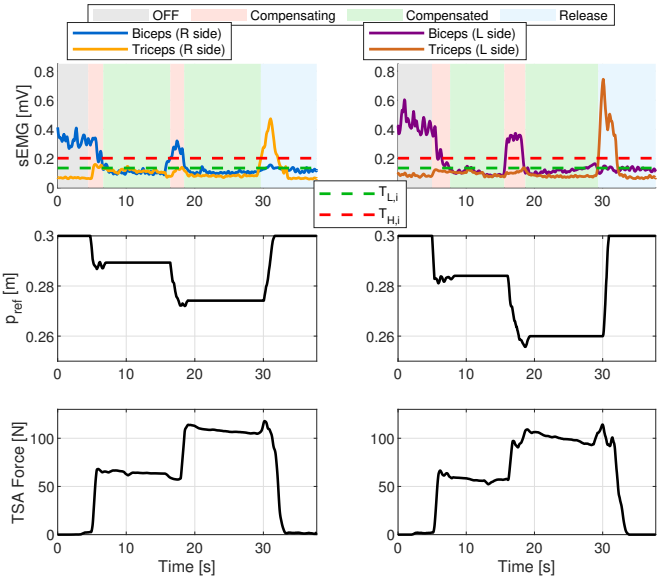

Fig. 6: *Highlighted case* of the dual arm experiment with simultaneous load compensations, for the subject U1. Colored areas: 'OFF' indicates the not powered situation, 'Compensating' the active assistance phase, 'Compensated' the phase in which the sEMG reached the requested value and 'Release' the loads removed phase.

the higher threshold $T_{H,b}$ for both arms. Then, around time $t = 5s$ the system was activated and, consequently, the sEMG-driven controller made the assistive support increase in such a way that the biceps sEMG activity decreased until it reached the lower threshold $T_{L,b}$ (red-coloured zone in Fig. 6). In particular, this is visible observing the decreasing, always at $t = 5s$, of the string lengths p_{ref} (Fig. 6, middle row) according to eq. (1) and Fig. 3, which in turn produced the increasing of the force provided by the TSA modules, as visible in the force sensor measurements reported in the bottom row of Fig. 6. Thereafter, in proximity of the time $t = 15s$, the experimenter placed on the the top of the 2 kg box (already compensated) an identical box of 2 kg, therefore composing a new resulting box of 4 kg. In this relation, it is visible how the sEMG activity of the biceps surpassed again the value $T_{H,b}$, causing the controller adapt to this additional load to be compensated, and therefore decreasing p_{ref} (and consequently increasing the TSA module force) to a new value, determined by the decreasing of the biceps activity until it reached, again, the value of $T_{L,b}$. At this point, the 4 kg box is compensated (green-coloured zone in Fig. 6) and the subject could sustain the total weight with basically no effort. Finally, the experimenter removed the entire load: this, in practice, required the subject to "push toward down" with his forearm in order to keep the position with the elbow flexed at 90°, causing an increase of the triceps sEMG signal (around time $t = 29s$, blue-coloured zone in Fig. 6) over the higher threshold $T_{H,t}$ for both arms. This rapidly determined an increase of the p_{ref} values and TSA forces. At time $t = 31s$ the string lengths were back to the initial value: no support was provided since no muscle activity was present, until a new load was added again.

Fig. 7a, 7b and 7c report single arm compensation of 1 kg, 2 kg and 3 kg, respectively (see Sec. IV-A); the string

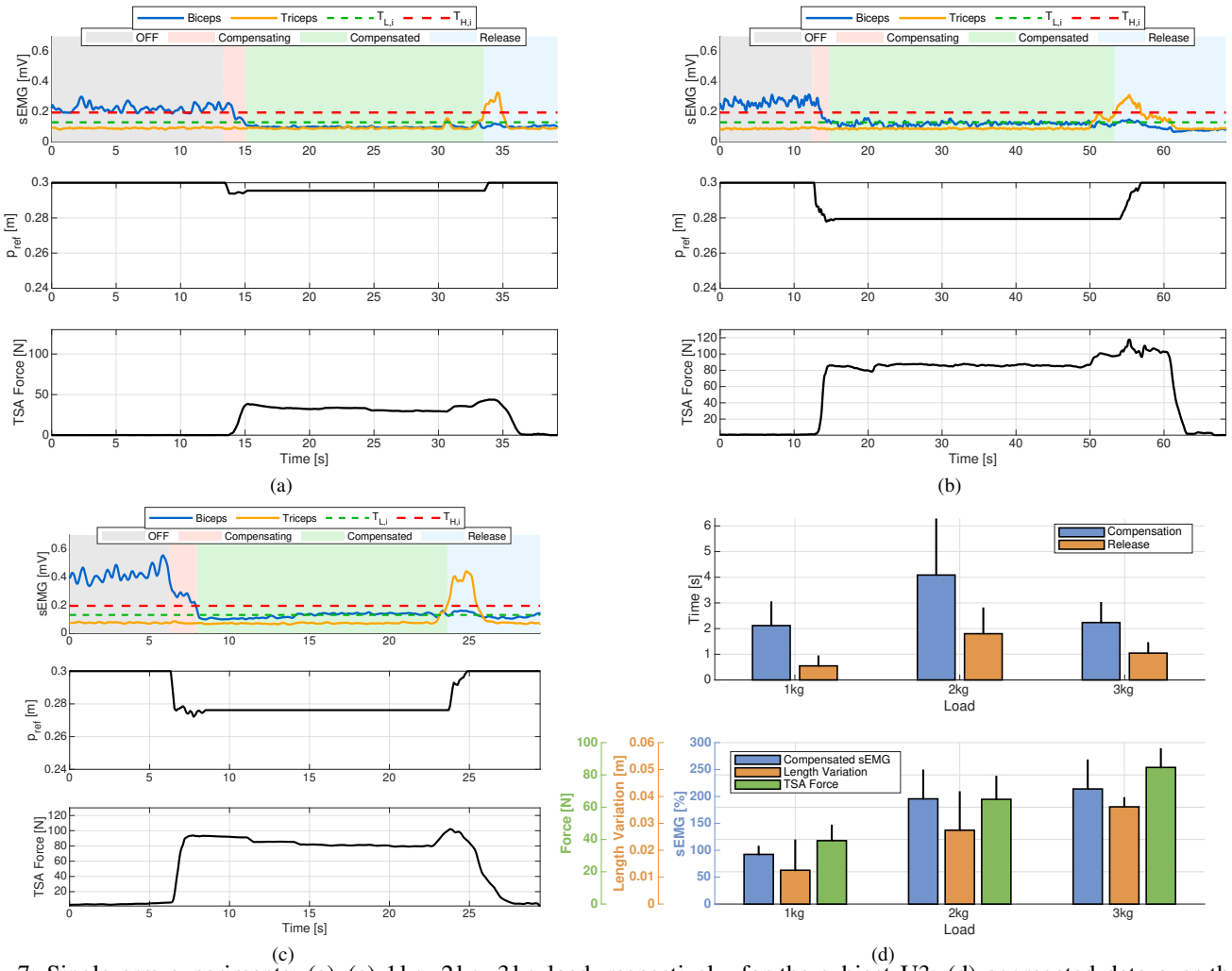

Fig. 7: Single arm experiments: (a)–(c) 1 kg, 2 kg, 3 kg load, respectively, for the subject U3; (d) aggregated data over the 4 subjects (mean values and standard deviation). For more details on the colored areas legend refer to Fig. 6.

length p_{ref} and related forces increased (red-coloured zones), assisting the biceps activity and compensating the load. This held for the green-coloured zones, until the removal of the load generated an increasing in the activity of the triceps (blue-coloured zones), bringing back the system to the initial state of no support – in accordance with the concepts previously outlined for the *highlighted case* (i.e., Fig. 6). The described behaviour was successfully reported by all the subjects, and related aggregated results are reported in Fig. 7d. In particular, in the top graph of Fig. 7d it is possible to observe that the mean time (over the subjects) requested for the load compensation and for the "release" phase (i.e. the removal of the load and coming back to the no support situation – the blue-coloured zones) were less than 5s, with a much lower mean time of the release with respect to the compensation. Additionally, in the bottom graph of Fig. 7d it is clearly visible the increasing trend – with respect to the increasing of the load from 1 kg to 3 kg – of: *(i)* the mean percentage of compensated sEMG activity computed with respect to the value $T_{L,b}$, *(ii)* the mean variation of the TSA module string length and *(iii)* the mean force provided by the TSA module.

Fig. 8a is related to the task with the 1 kg and 3 kg loads applied on the right and left arms, respectively, for the subject U1, and Fig. 8b to the same task but with inverted arm sides for the 1 kg and 3 kg loads, for the subject U3 (see Sec. IV-A, Fig. 5b,5c.) Specifically, in such figures, it is visible how the load compensation was turned on at different times for the two arms (different temporal lengths of the gray-coloured zones for the right and left arms). On the other hand, the activation of the triceps activities occurred almost at the same time for the left and right arms, around $t = 65s$ for U1 and $t = 40s$ for U3 (green- and blue-coloured zones), due to a simultaneous load removal on the right and left sides. The decoupled dual arm tasks were successfully performed by all the subjects, with comparable mean times for the compensation of the loads and for the release phase between the right and left arm sides, as it is shown in Fig. 8c. Also, it is possible to see how the mean percentage of the compensated sEMG activity (computed with respect to the value $T_{L,b}$) was higher for the right arm, due to a higher level of the sEMG signal of the right side biceps for some subjects.

Fig. 9 reports the results for the dual arm experiment with the simultaneous compensation of the box-like load for the two arms (Fig. 5d-5e): Fig. 9a reports the behaviour that has been highlighted in Fig. 6 and already discussed in detail in the previous subsection. In this experiment, the task involved also the use of the wrist joint. Please note that the support provided by the ExoSuit to the forearm does not affect the muscle

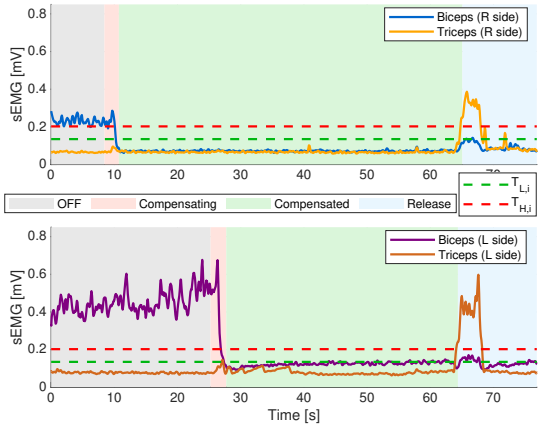

(a)

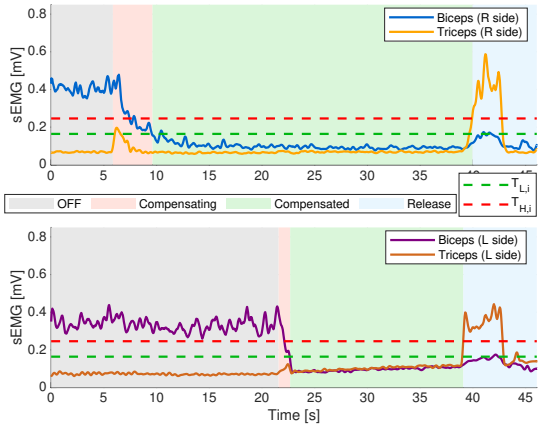

(b)

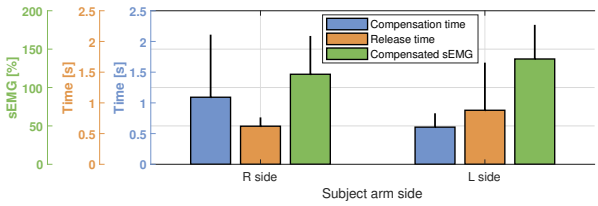

(c)

Fig. 8: Dual arm experiments with decoupled compensation: (a),(b) subjects U1 and U3, respectively; (c) aggregated results over the 4 subjects (mean value and standard deviation). For more details on the colored areas legend refer to Fig. 6.

activity related to the wrist. Additionally, Fig 9b reports the aggregated results for all subjects, comparing the application of the first 2 kg box-like load with its subsequent increasing to 4 kg. Particularly, the mean time for the sEMG compensation was higher for the 4 kg load, while, at the same time, the mean percentage of compensated sEMG was lower for the 2 kg load: ExoSuit was enabled to provide support when the 2 kg load was *already* applied, while the variation of the load from 2 kg to 4 kg occurred *during the functioning* of the assistive device.

Fig. 10 reports on the dynamic dual arm task (lowering-lifting task of the 2 kg box-like load) (see Sec. IV-A and Fig. 5d), for the subject U1. Referring to the red-coloured zone, an increase of the TSA string lengths (p_{ref}), and related forces, can be observed, in accordance to the load compensation for the assistance of biceps sEMG – in this phase both forearms are flexed at 90^o. Thereafter, the situation remained unchanged

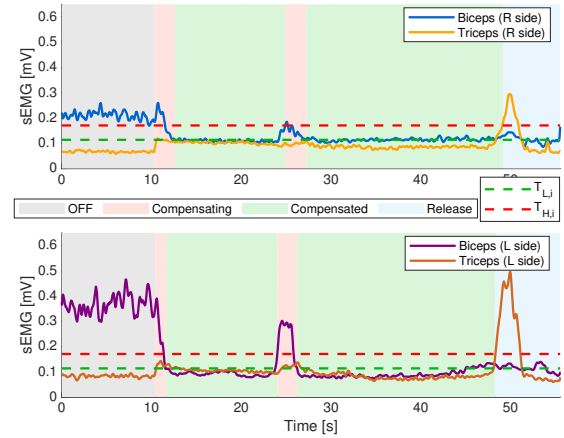

(a)

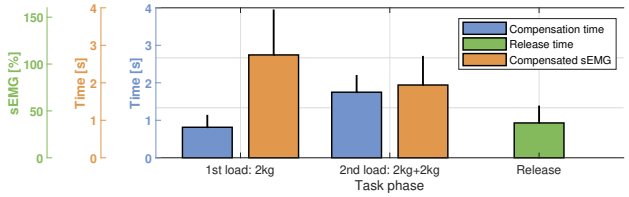

(b)

Fig. 9: Dual arm experiments with simultaneous compensation: (a) subject U3; (b) aggregated results over the 4 subjects (mean value and standard deviation). For more details on the colored areas legend refer to Fig. 6.

(green-coloured zone) until the subject extended both forearms in order to lower the held box (blue-coloured zones), followed by a load lifting (forearms flexion yellow-coloured zones), repeated twice. For the lowering of the load, the subject produced a downward push, which in turn generates a triceps sEMG increase, enabling – as far as the triceps activity reached the value $T_{H,t}$ – the load lowering motions (around t = 20 s and 40 s). The lifting actions of the subject generated a biceps activity rise, allowing the onset of the load lifting motions (around t = 30 s and 50 s) in conjunction with the reaching of the value $T_{H,b}$ by the biceps sEMG. During this dynamic task, it is possible to observe how the biceps/triceps activities were limited by the threshold values thanks to the support provided by the ExoSuit: a surpassing of the thresholds was necessarily present for (and bounded to) the onset of the lowering/lifting motions, but still restricted close to the value T_H. This behaviour was confirmed for all subjects, as illustrated by the aggregated results of Fig. 11, which reports the boxplots of the subjects mean biceps (top graph) and triceps (bottom graph) activity computed over the task zones of Fig. 10. Note that, in Fig. 11, the sEMG (and the thresholds) of each subject are normalized with respect to the subject-related threshold values $T_{L,i}$, $i = \{b,t\}$ (we refer to this normalized data as T_L-normalized), in order to compare the data among different subjects on single graphs.

V. CONCLUSION

In this paper, we present and evaluate an sEMG-driven soft ExoSuit based on the TSA system for both single and dual-arm assistive applications. The proposed system benefits from two independent twisted string actuators to perform the load compensation tasks. An sEMG-based controller has been

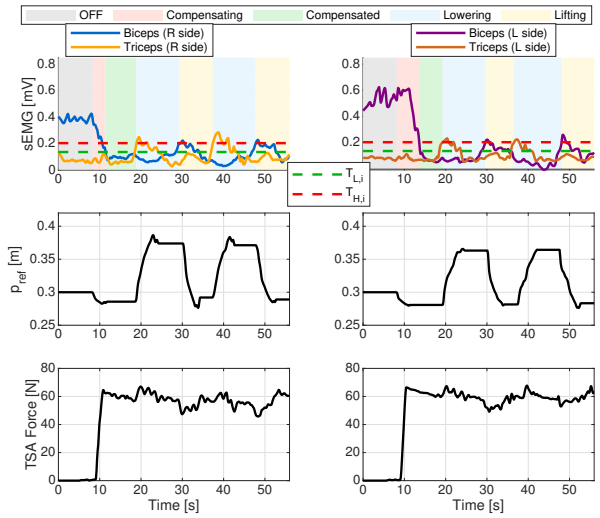

Fig. 10: Lowering-lifting experiment of the subject U1.

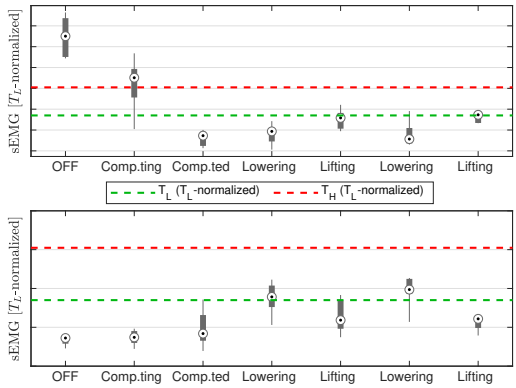

Fig. 11: Lowering-lifting experiments: mean sEMG over the 4 subjects (boxplot) for the task zones of Fig. 10.

implemented to compensate the user's muscle activities during applying and removing loads, using both biceps and triceps sEMG. Future work will be devoted to more complex assistive tasks that include additional degrees of freedom and ranges of motion.

REFERENCES

[1] A. Ebrahimi, D. Gröninger, R. Singer, and U. Schneider, "Control parameter optimization of the actively powered upper body exoskeleton using subjective feedbacks," in *Proc. IEEE Int. Conf. on Control, Automation and Robotics*, 2017, pp. 432–437.

[2] B. Kim and A. D. Deshpande, "An upper-body rehabilitation exoskeleton harmony with an anatomical shoulder mechanism: Design, modeling, control, and performance evaluation," *The International Journal of Robotics Research*, vol. 36, no. 4, pp. 414–435, 2017.

[3] R. Gopura, D. Bandara, K. Kiguchi, and G. K. Mann, "Developments in hardware systems of active upper-limb exoskeleton robots: A review," *Robotics and Autonomous Systems*, vol. 75, pp. 203–220, 2016.

[4] M. Wehner, B. Quinlivan, P. M. Aubin, E. Martinez-Villalpando, M. Baumann, L. Stirling, K. Holt, R. Wood, and C. Walsh, "A lightweight soft exosuit for gait assistance," in *Proc. IEEE Int. Conf. on Robotics and Automation*, 2013, pp. 3362–3369.

[5] V. Oguntosin, W. S. Harwin, S. Kawamura, S. J. Nasuto, and Y. Hayashi, "Development of a wearable assistive soft robotic device for elbow rehabilitation," in *Proc. IEEE Int. Conf. on Rehabilitation Robotics*, 2015, pp. 747–752.

[6] M. Xiloyannis, D. Chiaradia, A. Frisoli, and L. Masia, "Physiological and kinematic effects of a soft exosuit on arm movements," *Journal of neuroengineering and rehabilitation*, vol. 16, no. 1, p. 29, 2019.

[7] Y. Ding, I. Galiana, A. T. Asbeck, S. M. M. De Rossi, J. Bae, T. R. T. Santos, V. L. de Araújo, S. Lee, K. G. Holt, and C. Walsh, "Biomechanical and physiological evaluation of multi-joint assistance with soft exosuits," *IEEE Transactions on Neural Systems and Rehabilitation Engineering*, vol. 25, no. 2, pp. 119–130, 2017.

[8] M. Grimmer, B. T. Quinlivan, S. Lee, P. Malcolm, D. M. Rossi, C. Siviy, and C. J. Walsh, "Comparison of the human-exosuit interaction using ankle moment and ankle positive power inspired walking assistance," *Journal of biomechanics*, vol. 83, pp. 76–84, 2019.

[9] Y. Ding, I. Galiana, A. Asbeck, B. Quinlivan, S. M. M. De Rossi, and C. Walsh, "Multi-joint actuation platform for lower extremity soft exosuits," in *Proc. IEEE Int. Conf. on Robotics and Automation*, 2014, pp. 1327–1334.

[10] J. Bae, S. M. M. De Rossi, K. O'Donnell, K. L. Hendron, L. N. Awad, T. R. T. Dos Santos, V. L. De Araujo, Y. Ding, K. G. Holt, T. D. Ellis *et al.*, "A soft exosuit for patients with stroke: Feasibility study with a mobile off-board actuation unit," in *Proc. IEEE Int. Conf. on Rehabilitation Robotics*, 2015, pp. 131–138.

[11] G. Palli, C. Natale, C. May, C. Melchiorri, and T. Wurtz, "Modeling and control of the twisted string actuation system," *IEEE/ASME Transactions on Mechatronics*, vol. 18, no. 2, pp. 664–673, 2013.

[12] G. Palli, C. Melchiorri, G. Vassura, U. Scarcia, L. Moriello, G. Berselli, A. Cavallo, G. De Maria, C. Natale, S. Pirozzi *et al.*, "The dexmart hand: Mechatronic design and experimental evaluation of synergy-based control for human-like grasping," *The International Journal of Robotics Research*, vol. 33, no. 5, pp. 799–824, 2014.

[13] I. Gaponov, D. Popov, S. J. Lee, and J.-H. Ryu, "Auxilio: a portable cable-driven exosuit for upper extremity assistance," *Int. J. of Control, Automation and Systems*, vol. 15, no. 1, pp. 73–84, 2017.

[14] M. Hosseini, Y. Pane, A. Sengül, J. De Schutter, and H. Bruyninckx, "A novel haptic glove (exoten-glove) based on twisted string actuation (tsa) system for virtual reality," in *Int. Conf. on Human Haptic Sensing and Touch Enabled Computer Applications*, 2018, pp. 612–622.

[15] T. Sonoda and I. Godler, "Multi-fingered robotic hand employing strings transmission named twist drive," in *Proc. IEEE/RSJ Int. Conf. on Intelligent Robots and Systems*, 2010, pp. 2733–2738.

[16] I.-W. Park and V. SunSpiral, "Impedance controlled twisted string actuators for tensegrity robots," in *Proc. IEEE Int. Conf. on Control, Automation and Systems*, 2014, pp. 1331–1338.

[17] H. S. Lo and S. Q. Xie, "Exoskeleton robots for upper-limb rehabilitation: State of the art and future prospects," *Medical engineering & physics*, vol. 34, no. 3, pp. 261–268, 2012.

[18] K. Kiguchi, T. Tanaka, and T. Fukuda, "Neuro-fuzzy control of a robotic exoskeleton with EMG signals," *IEEE Transactions on Fuzzy Systems*, vol. 12, no. 4, pp. 481–490, 2004.

[19] K. Kiguchi and Y. Hayashi, "An EMG-based control for an upper-limb power-assist exoskeleton robot," *IEEE Transactions on Systems, Man, and Cybernetics, Part B: Cybernetics*, vol. 42, no. 4, pp. 1064–1071, 2012.

[20] Z. Li, B. Wang, F. Sun, C. Yang, Q. Xie, and W. Zhang, "SEMG-based joint force control for an upper-limb power-assist exoskeleton robot," *IEEE Journal of Biomedical and Health Informatics*, vol. 18, no. 3, pp. 1043–1050, 2014.

[21] M. Hosseini, R. Meattini, G. Palli, and C. Melchiorri, "A wearable robotic device based on twisted string actuation for rehabilitation and assistive applications," *Journal of Robotics*, vol. 2017, 2017.

[22] ——, "Development of sEMG-driven assistive devices based on twisted string actuation," in *Proc. IEEE Int. Conf. on Control, Automation and Robotics*, 2017, pp. 115–120.

[23] G. Palli, M. Hosseini, and C. Melchiorri, "A simple and easy-to-build optoelectronics force sensor based on light fork: Design comparison and experimental evaluation," *Sensors and Actuators A: Physical*, vol. 269, pp. 369–381, 2018.

[24] M. Hosseini, G. Palli, and C. Melchiorri, "Design and implementation of a simple and low-cost optoelectronic force sensor for robotic applications," in *Proc. IEEE Int. Conf. on Advanced Intelligent Mechatronics*, 2016, pp. 1011–1016.

[25] S. Benatti, B. Milosevic, F. Casamassima, P. Schönle, P. Bunjaku, S. Fateh, Q. Huang, and L. Benini, "Emg-based hand gesture recognition with flexible analog front end," in *Proc. IEEE Biomedical Circuits and Systems Conf.*, 2014, pp. 57–60.

[26] R. Meattini, M. Hosseini, G. Palli, and C. Melchiorri, "Early evaluation of semg-driven muscle modelling for rehabilitation and assistive applications based on wearable devices," in *Proc. IEEE Int. Conf. on Robotics and Biomimetics*, 2016, pp. 1480–1485.

[27] R. Meattini, G. Palli, and C. Melchiorri, "Experimental evaluation of a semg-based control for elbow wearable assistive devices during load lifting tasks," in *2017 International Conference on Rehabilitation Robotics (ICORR)*. IEEE, 2017, pp. 140–145.